Journal of Southeast University (English Edition) Vol. 38, No. 1, pp. 77 - 84 Mar. 2022 ISSN 1003—7985

Nitrate reduction by $\cdot CO_2^-$ from UV-activated HCOOH

Xu Yiqiao[1] Wu Lei[1] Zheng Tianyi[1,2]

([1]School of Energy and Environment, Southeast University, Nanjing 210096, China)

([2]Jiangsu Branch of China Municipal Engineering Northwest Design and Research Institute Co., Ltd., Nanjing 210017, China)

Abstract: To address the environmental and health hazards of nitrate (NO_3^-) in water, a denitrification advanced reduction process (ARP) using only formic acid (HCOOH) activated by ultraviolet (UV) light was proposed. The efficiency, influencing factors, mechanism, and kinetics of the reduction were investigated through component analysis and radical detection. Results show that, after 90 min of UV illumination, the reduction and gas conversion ratios of 50 mg/L NO_3^--N reach 99.9% and 99.8%, respectively, under 9 mM of C_0 (HCOOH), pH = 3.0, and N_2 aeration. Meanwhile, 96.7% of HCOOH is consumed and converted into gas. The NO_3^--N conversion process includes the transformation to NO_2^--N, followed by a further reduction to gas and a direct conversion into gas, introducing small amounts of nitrite and ammonia. The carbon dioxide anion radical ($\cdot CO_2^-$) from HCOOH/$HCOO^-$ is the principal cause of NO_3^--N reduction by UV/HCOOH/N_2 ARP. In contrast, $\cdot CO_2^-$ production is caused by the hydroxyl radical ($\cdot OH$). The NO_3^--N reduction efficiency is enhanced by the increase in the light intensity, considerably affected by the initial pH, and less affected by inorganic anions, including Cl^-, $H_2PO_4^-$, and HCO_3^-/CO_3^{2-}. The initial HCOOH concentration and light intensity are the main factors that influence the NO_3^--N reduction rate.

Key words: nitrate reduction; advanced reduction process; ultraviolet; HCOOH; $\cdot CO_2^-$

DOI: 10.3969/j.issn.1003-7985.2022.01.012

Nitrate (NO_3^-) is often the focus in the nitrogen (N) pollution investigation of surface water and shallow groundwater[1]. Due to its stability, NO_3^- degrades slowly under natural conditions, leading to massive and persistent accumulation[2]. Excess NO_3^- stimulates algal growth, resulting in eutrophication and hypoxia[3-4]. High NO_3^- concentrations in drinking water have also been linked to diabetes, spontaneous abortion, thyroid problems, and stomach cancer[5]. To ensure human health, the World Health Organization established the maximum contaminant level (MCL) of 50 mg/L for NO_3^- in drinking water; however, many countries have still exceeded this MCL for NO_3^- from drinking water sources in recent years[6-8]. To remove NO_3^- from water, chemical reduction methods with a fast reaction rate and easy operation are widely adopted. Conventional chemical denitrification includes metal reduction and catalytic reduction. Chemical reduction methods use iron[9], aluminum[10], zinc, and other zerovalent metal as electron donors, and conventional chemical denitrification combines catalysts (usually metal-doped or carbon-doped semiconductor materials[11]) and hole scavengers (usually hydrogen or formic acid [HCOOH]) to obtain electronic interaction and electron transfer. Current research on chemical denitrification mainly aims to control the direction and degree of NO_3^- reduction to avoid nitrite (NO_2^-) or ammonia (NH_3) formation and improve gaseous N selectivity.

Recently, advanced reduction processes (ARPs) that produce reducing radicals to destroy contaminants by activating reagents have been widely adopted in the field of water treatment. Compared with traditional chemical methods, ARPs have the advantages of higher removal efficiency, more stable performance over a wide pH range, and easier combination with ultraviolet (UV) disinfection[12-13]. NO_3^- has been proven to be removable by UV/$S_2O_4^{2-}$ ARP according to Bensalah et al.[14], but sulfur and ammonium were introduced to the system. A suitable ARP for NO_3^- removal from drinking water should ensure that the products of reducing radicals are ultimately removed as well, and the carbon dioxide anion radical ($\cdot CO_2^-$) generated from organic acids or salts is an appropriate choice. $\cdot CO_2^-$ is a strongly reducing radical with a REDOX potential of $E(CO_2/\cdot CO_2^-) = -1.9$ V[15]. After being oxidized, $\cdot CO_2^-$ is converted into CO_2 that easily discharges into the atmosphere. HCOOH is regarded as the most favorable $\cdot CO_2^-$ provider because of its simple carboxylic acid structure[16]. Gu et al.[17] developed UV/$S_2O_8^{2-}$/HCOOH ARP for carbon tetrachloride degradation, through which $\cdot CO_2^-$ was rapidly produced. Chen et al.[18] adopted UV/H_2O_2/HCOOH for NO_3^- reduction and achieved approximately 100% NO_3^- removal, as well as a maximum gaseous N product selectivity of 80%.

Received 2021-09-14, **Revised** 2021-12-15.

Biographies: Xu Yiqiao (1998—), female, graduate; Wu Lei (corresponding author), male, associate professor, wulei@seu.edu.cn.

Foundation item: The National Major Science and Technology Project (No. 2017ZX07202-004-005).

Citation: Xu Yiqiao, Wu Lei, Zheng Tianyi. Nitrate reduction by $\cdot CO_2^-$ from UV-activated HCOOH[J]. Journal of Southeast University (English Edition), 2022, 38(1): 77 - 84. DOI: 10.3969/j.issn.1003-7985.2022.01.012.

Inspired by the aforementioned systems, this study aims to develop a highly efficient denitrification process utilizing ARPs without producing other pollutants. Herein, a simple system with UV as the activation method and HCOOH alone as the reducing agent was established.

1 Materials and Methods

1.1 Chemicals

HCOOH, sodium nitrate, and phosphate were purchased from Tianjin Kemiou Chemical Reagent Co., Ltd. (Tianjin, China). 5, 5-Dimethyl-1-pyrrolidine N-oxide(DMPO) was purchased from Aladdin (Shanghai, China). The other chemicals, such as potassium chloride, potassium bicarbonate, and potassium dihydrogen phosphate, were provided by Sinopharm Group Chemical Reagent Co., Ltd. (Shanghai, China). All chemicals were of analytical grade.

1.2 Experimental procedures

Experiments were conducted in a 250 mL quartz photochemical reactor with an inner condensing trap. All solutions were prepared with deionized deoxygenated water with a resistivity of more than 18 MΩ at room temperature. The initial concentration of NO_3^--N was 50 mg/L (3.57 mmol/L). Solutions were first aerated with N_2 or O_2 for five min and then subjected to the REDOX reaction under UV light. UV irradiation was conducted using high-pressure mercury lamps emitting polychromatic UV light between 200 and 650 nm. The lamps were warmed up for 15 min to reach a constant output before starting the irradiation experiments. Samples were taken every 15 min, and the reaction duration was 90 min.

1.3 Analytical methods

The analysis of N-containing compounds was performed using a UV-visible spectrophotometer (UV-1800PC) according to the national standards HJ/T 346—2007 (NO_3^-), GB 7493—1987 (NO_2^-), HJ 535—2009 (NH_3), and HJ 636—2012. Total organic carbon (TOC) was measured using a TOC analyzer (OLTOC1030W). The concentration of HCOOH was measured by sodium hydroxide titration. Radicals were detected by electron paramagnetic resonance (EPR) with a Bruker A300 EPR spectrometer. Each sample was mixed with the spin trapping agent DMPO and injected into capillary tubes with puncture needles for detection.

2 Results and Discussion

2.1 NO_3^- reduction efficiency by UV/HCOOH/N_2

The denitrification efficiencies of UV/HCOOH/N_2, UV/HCOOH/O_2, and UV/HCOOH were compared. The initial concentration of HCOOH was 10 mmol/L, and the power input of UV light was 125 W. The initial dissolved oxygen (DO) concentration of the solution was less than 0.1 mg/L under N_2 aeration, 26.0 mg/L under O_2 aeration, and 7.8 mg/L without aeration. The removal ratio of NO_3^--N at 90 min was 100%, 93.7%, and 98.9%. Reducing radicals can be rapidly consumed by O_2, leading to a decrease in the NO_3^--N removal ratio as the DO concentration increases. This finding indicates that the reducing atmosphere promotes NO_3^--N reduction. Therefore, the basic condition in this study was determined to be UV/HCOOH/N_2.

Then, the effect of the initial HCOOH concentration (C_0) on denitrification was investigated for optimal dosage determination, and the results are presented in Fig. 1. As the C_0(HCOOH) concentration increased from 1 mol/L to 9 mmol/L, the reduction ratio of NO_3^--N increased from 22.4% to 98.7% within 60 min, and the gas conversion ratio increased from 1.0% to 97.6%. At the end of the reaction, the reduction and gas conversion ratios of NO_3^--N were 99.9% and 99.8%, respectively, with C_0(HCOOH) = 9 mM, which was the highest. The reduction and gas conversion ratios were numerically similar, indicating that the dominant product of reduced NO_3^- was gas.

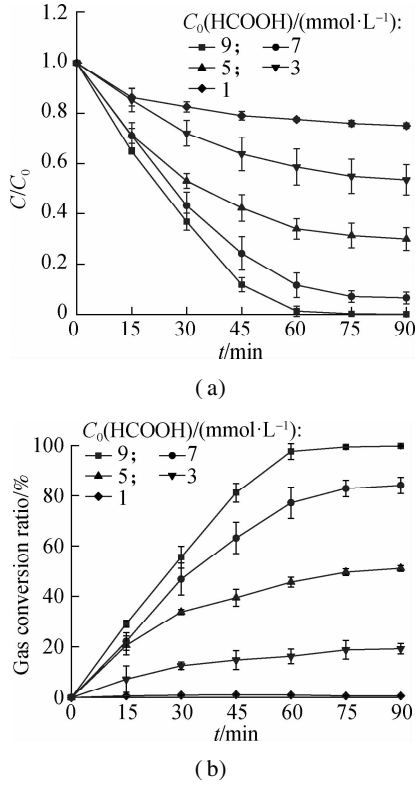

Fig. 1 Effect of C_0(HCOOH) concentration on NO_3^--N reduction. (a) Reduction ratio; (b) Gas conversion ratio

2.2 Safety evaluation of UV/HCOOH/N_2

The TOC concentration and the residual HCOOH concentration were detected for toxicity evaluation. Fig. 2(a) presents the dramatic decrease in TOC concentration with time under different C_0(HCOOH) concentrations, indica-

ting that HCOOH was depleted continuously with gas as the dominant product. When the C_0(HCOOH) concentration was less than 7 mmol/L, the eventual TOC concentration was lower than the limit set in the Hygienic Standard for Drinking Water (GB 5749—2006; i.e., 5 mg/L), and the highest NO_3^--N removal and gas conversion ratios reached 93.5% and 84.2%, respectively. When the C_0(HCOOH) concentration was 9 mmol/L, the removal and gas conversion ratios exceeded 99.8%, but the final TOC concentration was the highest (i.e., 11.9 mg/L). In short, NO_3^- reduction by UV/HCOOH/N_2 ARP involves the risk of secondary pollution. If the requirement for NO_3^- removal is strict, then excessive HCOOH may cause the TOC concentration in the solution at the end of the reaction to exceed the limit of the sanitary standards for domestic drinking water.

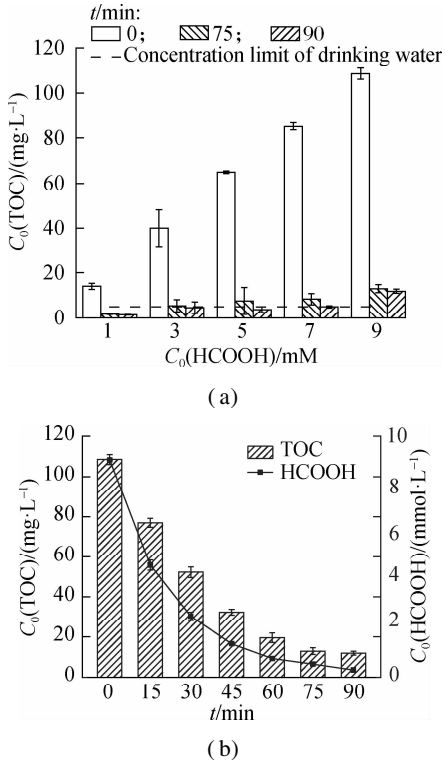

Fig. 2 TOC and HCOOH evaluation. (a) TOC concentration under different C_0(HCOOH) concentrations; (b) TOC and residual HCOOH concentrations when C_0(HCOOH) = 9 mM

To guarantee the reduction effect, the C_0(HCOOH) concentration used in subsequent studies was 9 mmol/L, and the trends of the TOC and HCOOH concentrations were further analyzed (see Fig. 2(b)). At the end of UV illumination, more than 96.7% of HCOOH was consumed, and the residual HCOOH concentration was at a negligible level (0.3 mmol/L).

2.3 Reaction mechanism analysis

In addition to gas, the possible by-products of NO_3^- in the UV/HCOOH/N_2 reduction process include NO_2^- and NH_3. Thus, their formation was quantitatively analyzed.

Fig. 3 shows that NO_2^--N accumulated during the NO_3^- reduction process. As the C_0(HCOOH) concentration increased, the concentration of NO_2^--N gradually decreased at 90 min of the reaction, indicating that part of NO_3^--N participated in the reduction reaction to produce NO_2^--N and was further reduced. NO_2^--N production showed a trend of first increasing and then decreasing, except at C_0(HCOOH) = 3 mmol/L, peaking at 60, 45, and 30 min.

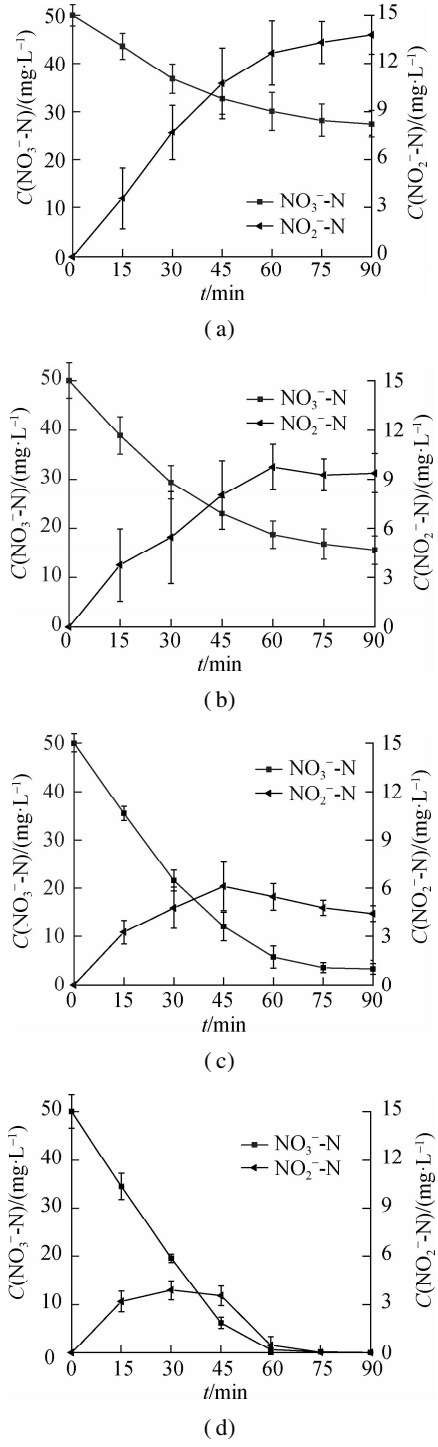

Fig. 3 NO_2^--N formation from NO_3^--N reduction. (a) C_0(HCOOH) = 3 mmol/L; (b) C_0(HCOOH) = 5 mmol/L; (c) C_0(HCOOH) = 7 mmol/L; (d) C_0(HCOOH) = 9 mmol/L

With C_0 (NO_3^--N) = 50 mg/L and C_0 (HCOOH) = 9 mmol/L, the highest NO_2^--N concentration (i.e., 3.9 mg/L) was achieved at 30 min. As the reaction proceeded, NO_2^- began to degrade, and its concentration decreased accordingly. Complete NO_2^--N degradation was reached at 90 min. Consequently, NO_3^- reduction by UV/HCOOH/N_2 ARP did not induce NO_2^- pollution.

NH_3-N generation is shown in Fig. 4. HCOOH dosage had a certain influence on the amount of NH_3-N. However, in general, NH_3-N concentration remained at a low level and tended to reach a certain value. This finding indicates that NH_3 is irreversible in the NO_3^- reduction process, thus determining the final denitrification and gas conversion efficiencies. When the C_0(HCOOH) concentration was 9 mM, the NH_3 concentration was always less than 0.3 mg/L. At 90 min, when the degradation of NO_3^- and NO_2^- was completed, NH_3-N production was less than 0.6%.

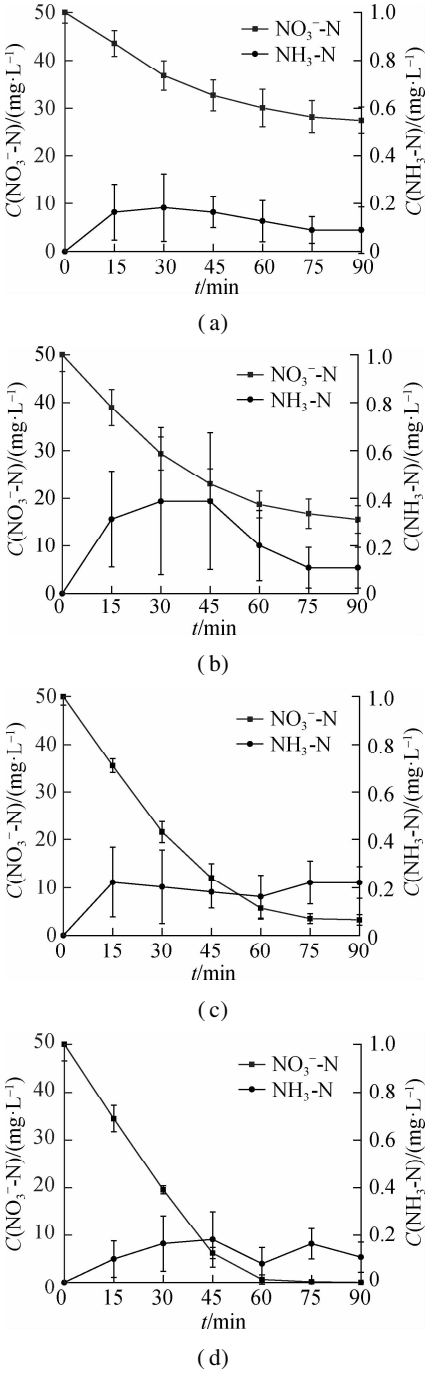

Fig. 4 NH_3-N formation from NO_3^--N reduction. (a) C_0 (HCOOH) = 3 mmol/L; (b) C_0 (HCOOH) = 5 mmol/L; (c) C_0 (HCOOH) = 7 mmol/L; (d) C_0(HCOOH) = 9 mmol/L

NO_3^- was replaced with NO_2^- of equal molar concentration for further mechanism analysis. Under 9 mM of HCOOH, the reduction rate of NO_2^--N was higher than that of NO_3^--N (nearly complete within 30 min), but more by-products were generated. As shown in Fig. 5 (a), the decrease in the concentration of NO_2^--N was accompanied by the formation of NH_3, the concentration of which reached the highest value (i.e., 4.2 mg/L) at 45 min and tended to maintain a constant value (i.e., 3.1 mg/L) at the end of the reaction. The production and accumulation of NH_3 indicated that NO_2^- was not the only product of the first conversion of NO_3^- in NO_3^--N reduction by UV-activated HCOOH. The direct conversion of NO_3^--N into gas also occurred.

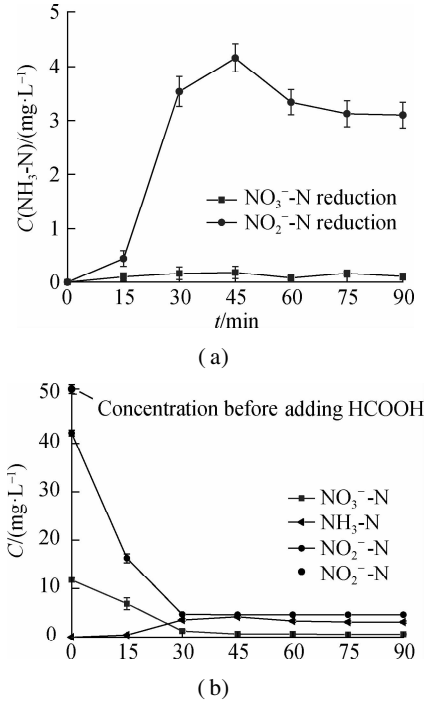

Fig. 5 NO_2^- reduction by UV/HCOOH. (a) NH_3-N formation compared with NO_3^-; (b) NO_2^--N reduction products

Fig. 5(b) illustrates the existence of a certain amount of NO_3^--N before the reaction started, and the NO_3^--N concentration gradually decreased as the reaction proceeded. The NO_2^--N concentration decreased by approximately 20% after the addition of HCOOH, and the sum of this concentration and the NO_3^--N concentration was nearly equal to the concentration of NO_2^--N in the solution before the addition of HCOOH. The possible reason is that the solution became acidic after the addition of HCOOH, and NO_2^--N tended to decompose under acidic

conditions, producing NO_3^--N. To confirm this finding, a parallel experiment was conducted to replace HCOOH with HCl, the pH was adjusted to 3.0, and a similar concentration ratio of NO_2^- and NO_3^- was observed.

HCOOH, HCOOH/NO_3^--N, and HCOOH/C_3H_8O were subjected to in situ illumination and characterized by EPR for radical detection. HCOOH alone and HCOOH/NO_3^--N showed no signal peak in darkness (see Figs. 6 (a) and (b)). After UV illumination, the signal peak (m(H) = 19.1 g, m(N) = 15.8 g) of DMPO-$\cdot CO_2^-$ [19] appeared in both systems (see Figs. 6(c) and (d)), confirming the generation of $\cdot CO_2^-$. The peak intensity of the UV/HCOOH/NO_3^--N system was low because of the reaction between $\cdot CO_2^-$ and NO_3^--N. Figs. 6(e) and (f) show the EPR detection of hydroxyl radical ($\cdot$OH) from UV/HCOOH/C_3H_8O and HCOOH/C_3H_8O, respectively. A signal peak with the strength of 1:2:2:1 appeared in the UV/HCOOH system, proving the existence of $\cdot$OH[20-21]. After the addition of isopropanol as $\cdot$OH quencher, the signal peak of $\cdot$OH weakened evidently because of the consumption of radicals by the quencher. This finding coincides with that reported by Harbour et al. [19], which confirmed that $\cdot CO_2^-$ generation was caused by $\cdot$OH.

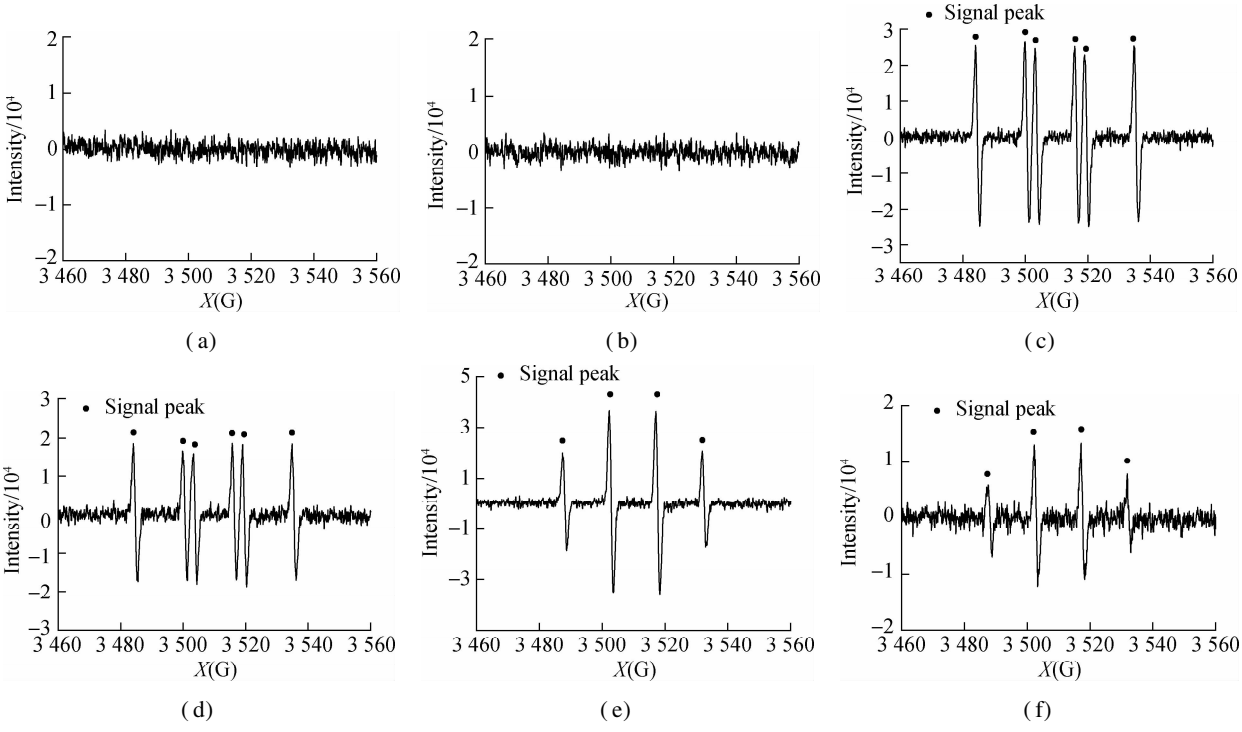

Fig. 6 EPR spectra of radicals. (a) DMPO-$\cdot CO_2^-$ from UV/HCOOH; (b) DMPO-$\cdot CO_2^-$ from UV/HCOOH/NO_3^--N; (c) DMPO-$\cdot$OH from UV/HCOOH; (d) DMPO-$\cdot$OH from UV/HCOOH/C_3H_8O; (e) HCOOH; (f) HCOOH/NO_3^--N

From the previously presented discussion, the reaction paths of NO_3^- reduction by UV-activated HCOOH are proposed in Fig. 7.

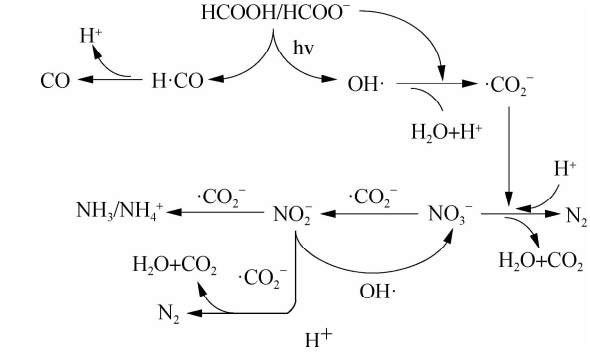

Fig. 7 Conceptual reaction mechanism of UV-activated HCOOH denitrification

2.4 Effects of some factors on NO_3^- reduction

High-pressure mercury lamps with light intensities of 125, 175, and 250 W were selected to investigate the effect of light intensity. After 45 min of irradiation, the reduction ratios of NO_3^--N at 125, 175, and 250 W were 88.2%, 97.8%, and 99.0%, respectively. This finding can be attributed to the enhancement of light intensity that accelerates the photon excitation rate of HCOOH to produce $\cdot$OH, thus generating more $\cdot CO_2^-$. At the end of the reaction, the reduction rates of NO_3^--N at three light intensities all exceeded 99.9%.

Six pH gradients, i.e., 2.0, 4.0, 6.0, 8.0, 10.0, and unadjusted pH (i.e., 3.0), were applied to verify the effect of pH on $\cdot CO_2^-$ denitrification. Fig. 8 illustrates that, at 90 min, the NO_3^- reduction ratio (i.e., 99.9%) and gas conversion ratio (i.e., 99.8%) both peaked under unadjusted pH (i.e., 3.0). When the pH increased to 4.0, the reduction and gas conversion ratios of NO_3^--N still reached high levels at the end of the reaction (i.e., 98.6% and 98.2%, respectively) with a slight decrease in the reduction rate. When the initial pH

successively increased to 6.0, 8.0, and 10.0, the reduction efficiency and gas conversion ratio of NO_3^--N remarkably decreased. Given that pK_a(HCOOH) = 3.75 when pH > 3.75, the main existing form of HCOOH is $HCOO^-$, whose ability to produce $\cdot CO_2^-$ under UV irradiation is weak, thus inhibiting the reduction of NO_3^--N. At pH = 2.0, the removal and gas conversion ratios of NO_3^--N after 90 min were the lowest, i.e., 80.2% and 69.2%, respectively. The decomposition of REDOX-active groups in the solution under a hyperacid environment can explain the decrease in the reduction effect.

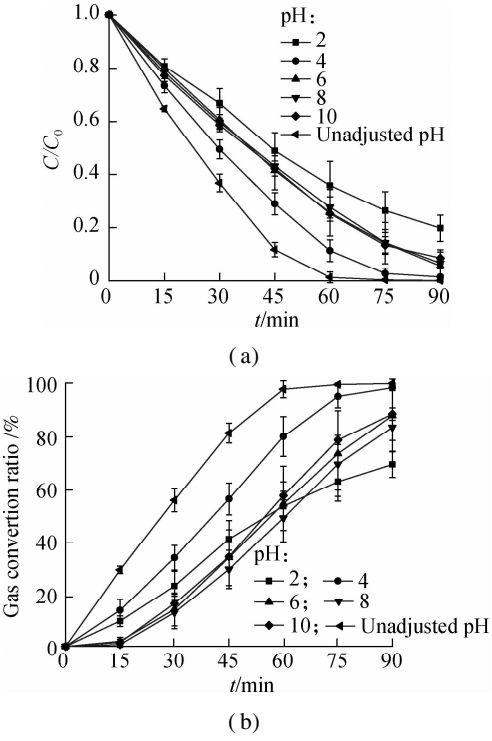

Fig. 8 Effects of pH on NO_3^--N reduction. (a) Reduction ratio; (b) Gas conversion ratio

Solution pH variation is shown in Fig. 9. When the initial pH was 2.0 and 10.0, the solution pH remained unchanged within 90 min. When the initial pH was 4.0, 6.0, 8.0, and unadjusted (i.e., 3.0), the solution pH increased with time and reached a certain value eventually, indicating that a large amount of HCOOH was consumed in the UV activation process, resulting in the solution pH changing to neutral and weakly alkaline.

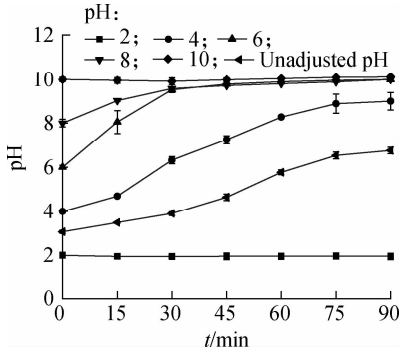

Fig. 9 pH variation with reaction time

Consequently, the initial pH is one of the main factors that influence the UV/HCOOH/N_2 denitrification system. The optimal pH is 3 to 4. Meanwhile, a hyperacid environment has an adverse effect on the reduction effect, and a neutral or alkaline environment also reduces the reduction effect but to a slight extent.

The influence of common anions in natural water wasinvestigated under a 125 W high-pressure mercury lamp. The concentration of anions was set at 1, 10, and 100 mmol/L.

Cl^- and $H_2PO_4^-$ showed no significant effect on NO_3^- reduction. As the initial anion concentration increased, the reduction rates slightly decreased. With Cl^- or $H_2PO_4^-$ of 100 mM, the final removal ratio of NO_3^--N could still reach 98.0% and 98.9%, respectively.

Fig. 10 shows that, after 90 min, the removal ratio of NO_3^--N showed only a slight change under 1 and 10 mM of HCO_3^- and a 3.5% decrease under 100 mM of HCO_3^-. The addition of HCO_3^- changed the initial pH to 3.27, 5.64, and 7.68. For the system with 100 mM of HCO_3^-, the initial pH was adjusted in the same way as when HCO_3^- was not added. Moreover, the comparison confirms that, under acidic conditions, NO_3^--N reduction was less inhibited when HCO_3^- was converted into CO_3^{2-}. Therefore, HCO_3^- can inhibit NO_3^--N reduction in two ways: 1) Under a high HCO_3^- concentration, the increase in the initial pH of the solution inhibits the reduction of NO_3^--N. 2) $\cdot OH$ yielded by UV – activated HCOOH reacts with HCO_3^- to produce CO_3^-, blocking the production of $\cdot OH$[22] as

$$\cdot OH + HCO_3^- \rightarrow H_2O + CO_3^- \quad (1)$$

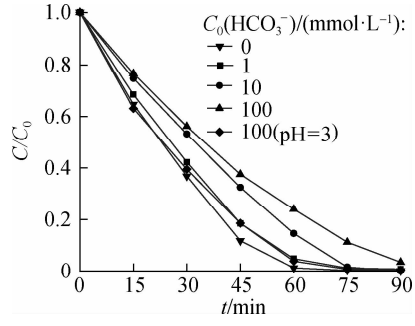

Fig. 10 Effects of HCO_3^- on NO_3^--N reduction

Furthermore, when the concentration of HCO_3^- further increases, it reacts with $\cdot CO_2^-$, as follows[23]:

$$\cdot CO_2^- + HCO_3^- \rightarrow HCO_2^- + \cdot CO_3^-$$

Therefore, the presence of HCO_3^- has a certain effect on the reduction of NO_3^--N.

2.5 Kinetic analysis

The kinetics of NO_3^--N reduction by UV/HCOOH/N_2 was analyzed for further interpretation. The sampling interval was reduced to 5 min, and the experiments were conducted with a thermostatic magnetic stirrer to stabilize the temperature at 25 ℃.

First, the reduction curve of NO_3^--N under a 125 W mercury lamp with C_0(HCOOH) = 9 mmol/L was fitted with C/C_0 and $\ln(C/C_0)$ with ordinate and reaction time as abscissa. The entire process can be divided into two stages; namely, a zero-order kinetic reaction in the early stage and first-order kinetic reaction in the late stage. In the first 30 min, the reduction process conformed to the zero-order reaction kinetics, and the corresponding zero-order rate constant was 1.03 min^{-1}. At the later stage, the NO_3^- reduction process fitted the first-order reaction equation, and the corresponding rate constant was 0.08 min^{-1}. The difference between the two stages was caused by the formation of NO_2^--N in the NO_3^--N reduction process.

The influence of C_0(HCOOH), initial pH, and light intensity on the NO_3^--N reduction kinetics was investigated. Due to the limitation of the NO_3^--N removal ratio, only zero-order kinetic fitting was conducted for degradation under different light intensities. The kinetic parameters shown in Tab. 1 indicate that C_0(HCOOH) and light intensity are the main factors that influence the NO_3^--N reduction rate. Meanwhile, the initial pH has a relatively minimal influence. The increase in C_0(HCOOH) concentration from 1 to 9 mM increased k_0 of the zero-order stage from 0.005 8 to 0.021 1 min^{-1} and k_1 of the first-order stage by 0.11 min^{-1}. When the light intensity increased to 175 and 250 W, k_0 increased to 0.026 and 0.043 min^{-1}, respectively.

Tab. 1 Kinetic parameters of NO_3^- reduction under different influencing factors

Factors	Value	Zero-order stage	R_0^2	First-order stage	R_1^2
C_0 (HCOOH)/(mmol·L^{-1})	1	$y=0.983\ 5-0.005\ 8x$	0.902 4	$y=0.156\ 0+0.001\ 54x$	0.947 3
	3	$y=0.997\ 4-0.009\ 3x$	0.999 0	$y=0.209\ 4+0.004\ 96x$	0.946 5
	5	$y=0.982\ 3-0.015\ 6x$	0.983 2	$y=0.409\ 9+0.009\ 63x$	0.916 2
	7	$y=0.998\ 0-0.018\ 9x$	0.999 7	$y=-0.045\ 8+0.033\ 4x$	0.945 2
	9	$y=0.987\ 8-0.021\ 1x$	0.995 5	$y=-2.416\ 5+0.109\ 5x$	0.991 2
UV intensity/W	125	$y=0.987\ 8-0.021\ 1x$	0.995 5	$y=-2.416\ 5+0.109\ 5x$	0.991 2
	175	$y=0.989\ 1-0.026\ 1x$	0.997 7		
	250	$y=1-0.043\ 2x$			
Initial pH	2	$y=0.992\ 1-0.011\ 2x$	0.996 6	$y=-0.188\ 4+0.020\ 2x$	0.999 7
	4	$y=0.985\ 1-0.015\ 8x$	0.996 6	$y=-1.912\ 0+0.070\ 2x$	0.982 0
	6	$y=0.997\ 0-0.013\ 0x$	0.999 8	$y=-1.203\ 1+0.044\ 0x$	0.976 7
	8	$y=0.987\ 4-0.012\ 6x$	0.996 6	$y=-1.118\ 5+0.041\ 6x$	0.986 9
	10	$y=0.983\ 4-0.012\ 8x$	0.994 5	$y=-0.758\ 2+0.036\ 1x$	0.995 6
	Unadjusted	$y=0.987\ 8-0.021\ 1x$	0.995 5	$y=-2.416\ 5+0.109\ 5x$	0.991 2

3 Conclusions

1) Under the basic conditions of 90 min of UV illumination, 9 mmol/L of C_0(HCOOH), and N_2 aeration, 99.9% of NO_3^--N could be removed, and the gas conversion ratio of NO_3^--N could reach 99.8%. The residual HCOOH concentration was negligible (i.e., 0.3 mmol/L).

2) NO_3^- reduction by UV/HCOOH/N_2 ARP was accompanied by the generation of NO_2^- and NH_3 but did not cause secondary N pollution at the end of the reaction. NO_2^- was eventually reduced and removed from the solution, and the concentration of NH_3 was always lower than 0.3 mg/L. The direct conversion of NO_3^--N into gas occurred during the reaction process in addition to the formation of NO_2^--N and subsequent reduction to gas.

3) EPR detection of in situ illumination proved that NO_3^--N reduction was caused by $\cdot CO_2^-$, and $\cdot CO_2^-$ generation was caused by $\cdot OH$.

4) The initial HCOOH concentration, UV light intensity, and initial pH were the main factors that influenced the UV/HCOOH/N_2 denitrification efficiency, and anions in natural water showed no significant effect on NO_3^- conversion.

References

[1] Pacheco F A L, Santos R M B, Fernandes L F S, et al. Controls and forecasts of nitrate yields in forested watersheds: A view over mainland Portugal[J]. *Science of the Total Environment*, 2015, **537**: 421 − 440. DOI: 10.1016/j.scitotenv.2015.07.127.

[2] Huno S K M, Rene E R, Van Hullebusch E D, et al. Nitrate removal from groundwater: A review of natural and engineered processes[J]. *Journal of Water Supply: Research and Technology—Aqua*, 2018, **67**(8): 885 − 902. DOI: 10.2166/aqua.2018.194.

[3] Blarasin M, Cabrera A, Matiatos I, et al. Comparative evaluation of urban versus agricultural nitrate sources and sinks in an unconfined aquifer by isotopic and multivariate analyses[J]. *Science of the Total Environment*, 2020, **741**: 140374. DOI: 10.1016/j.scitotenv.2020.140374.

[4] Chen N W, Peng B R, Hong H S, et al. Nutrient enrichment and N: P ratio decline in a coastal bay-river system in southeast China: The need for a dual nutrient (N and P) management strategy[J]. *Ocean & Coastal Management*, 2013, **81**: 7 − 13. DOI: 10.1016/j.ocecoaman.2012.07.013.

[5] Dan-Hassan M A, Olasehinde P I, Amadi A N, et al. Spatial and temporal distribution of nitrate pollution in groundwater of Abuja, Nigeria[J]. *International Journal of Chemistry*, 2012, **4**(3): 104 − 112. DOI: 10.5539/ijc.v4n3p104.

[6] Lotfata A, Ambinakudige S. Factors affecting the spatial pattern of nitrate contamination in Texas aquifers[J]. *Management of Environmental Quality: An International Journal*, 2019, **31**(4): 857 − 876. DOI: 10.1108/MEQ-

05-2019-0097.
[7] Vystavna Y, Diadin D, Grynenko V, et al. Determination of dominant sources of nitrate contamination in transboundary (Russian Federation/Ukraine) catchment with heterogeneous land use[J]. *Environ Monit Assess*, 2017, **189**: 509. DOI: 10.1007/s10661-017-6227-5.
[8] Yan B Z, Xiao C L, Liang X J, et al. Impacts of urban land use on nitrate contamination in groundwater, Jilin City, Northeast China[J]. *Arabian Journal of Geosciences*, 2016, **9**(2): 105. DOI: 10.1007/s12517-015-2052-8.
[9] Liu Y, Wang J L. Reduction of nitrate by zero valent iron (ZVI)-based materials: A review[J]. *Sci Total Environ*, 2019, **671**: 388 - 403. DOI: 10.1016/j.scitotenv.2019.03.317.
[10] Wang B Q, An B H, Liu Y, et al. Selective reduction of nitrate into nitrogen at neutral pH range by iron/copper bimetal coupled with formate/ferric ion and ultraviolet radiation[J]. *Separation and Purification Technology*, 2020, **248**: 117061. DOI: 10.1016/j.seppur.2020.117061.
[11] Liu H, Liu X Y, Yang W W, et al. Photocatalytic dehydrogenation of formic acid promoted by a superior PdAg@g-C_3N_4 Mott-Schottky heterojunction[J]. *Journal of Materials Chemistry A*, 2019, **7**(5): 2022 - 2026. DOI: 10.1039/c8ta11172c.
[12] Jung B, Safan A, Duan Y, et al. Removal of arsenite by reductive precipitation in dithionite solution activated by UV light[J]. *Journal of Environmental Sciences*, 2018, **74**: 168 - 176. DOI: 10.1016/j.jes.2018.02.023.
[13] Xiao Q, Wang T, Yu S L, et al. Influence of UV lamp, sulfur(IV) concentration, and pH on bromate degradation in UV/sulfite systems: Mechanisms and applications[J]. *Water Research*, 2017, **111**: 288 - 296. DOI: 10.1016/j.watres.2017.01.018.
[14] Bensalah N, Nicola R, Abdel-Wahab A. Nitrate removal from water using UV-M/$S_2O_4^{2-}$ advanced reduction process[J]. *International Journal of Environmental Science and Technology*, 2013, **11**(6): 1733 - 1742. DOI: 10.1007/s13762-013-0375-0.
[15] An B H, He H N, Duan B H, et al. Selective reduction of nitrite to nitrogen gas by CO_2 anion radical from the activation of oxalate[J]. *Chemosphere*, 2021, **278**: 130388. DOI: 10.1016/j.chemosphere.2021.130388.
[16] Tugaoen H O, Garcia-Segura S, Hristovski K, et al. Challenges in photocatalytic reduction of nitrate as a water treatment technology[J]. *Science of the Total Environment*, 2017, **599 - 600**: 1524 - 1551. DOI: 10.1016/j.scitotenv.2017.04.238.
[17] Gu X G, Lu S G, Fu X R, et al. Carbon dioxide radical anion-based UV/$S_2O_8^{2-}$/HCOOH reductive process for carbon tetrachloride degradation in aqueous solution[J]. *Separation and Purification Technology*, 2017, **172**: 211 - 216. DOI: 10.1016/j.seppur.2016.08.019.
[18] Chen J L, Liu J Y, Zhou J S, et al. Reductive removal of nitrate by carbon dioxide radical with high product selectivity to form N_2 in a UV/H_2O_2/HCOOH system[J]. *Journal of Water Process Engineering*, 2020, **33**: 101097. DOI: 10.1016/j.jwpe.2019.101097.
[19] Harbour J R, Hair M L. Spin trapping of the $\cdot CO_2^-$ radical in aqueous medium[J]. *Canadian Journal of Chemistry*, 2011, **57**(10): 1150 - 1152. DOI: 10.1139/v79-188.
[20] Cheng S A, Fung W K, Chan K Y, et al. Optimizing electron spin resonance detection of hydroxyl radical in water[J]. *Chemosphere*, 2003, **52**(10): 1797 - 1805. DOI: 10.1016/s0045-6535(03)00369-2.
[21] Han S K, Hwang T M, Yoon Y, et al. Evidence of singlet oxygen and hydroxyl radical formation in aqueous goethite suspension using spin-trapping electron paramagnetic resonance (EPR)[J]. *Chemosphere*, 2011, **84**(8): 1095 - 1101. DOI: 10.1016/j.chemosphere.2011.04.051.
[22] Augusto O, Bonini M G, Amanso A M, et al. Nitrogen dioxide and carbonate radical anion: Two emerging radicals in biology[J]. *Free Radical Biology and Medicine*, 2002, **32**(9): 841 - 859. DOI: 10.1016/S0891-5849(02)00786-4.
[23] Draganic Z D, Negronmendoza A, Sehested K, et al. Radiolysis of aqueous-solutions of ammonium bicarbonate over a large dose range[J]. *Radiation Physics and Chemistry*, 1991, **38**(3): 317 - 321. DOI: 10.1016/1359-0197(91)90100-G.

基于紫外光活化甲酸产生二氧化碳自由基的硝态氮还原分析

许贻乔[1] 吴 磊[1] 郑天怡[1,2]

([1] 东南大学能源与环境学院, 南京 210096)
([2] 中国市政工程西北设计研究院有限公司江苏分公司, 南京 210017)

摘要: 为解决水中硝态氮引发的环境和健康问题,提出了一种以甲酸为还原剂、以紫外光为活化手段的硝态氮还原(ARP)方法. 通过组分分析和自由基测定研究了体系的还原效能、影响因素、反应机理及反应动力学. 结果表明:在 C_0(HCOOH) = 9 mmol/L、初始 pH = 3.0 和 N_2 曝气条件下,紫外光照 90 min 后 50 mg/L 硝态氮的还原率和气体转化率分别达到 99.9% 和 99.8%,同时 96.7% 的甲酸被消耗并转化为气体. 该体系还原硝态氮的反应中不仅存在首先生成亚硝态氮再进一步被还原为气体的过程,还存在硝态氮直接转化为气体的过程. 硝态氮的还原主要由活化 $HCOOH/HCOO^-$ 产生的二氧化碳自由基($\cdot CO_2^-$)实现,而羟基自由基($\cdot OH$)是 $\cdot CO_2^-$ 的前体物. 硝态氮还原率随光照强度增加而提高,初始 pH 值对还原效果影响较大,而 Cl^-、$H_2PO_4^-$ 和 HCO_3^-/CO_3^{2-} 等无机阴离子的影响则较小. 甲酸初始浓度和紫外光强是还原速率的主要影响因素.

关键词: 硝态氮还原;高级还原技术;紫外光;甲酸;二氧化碳自由基
中图分类号: X52